

S. TOMASIK^{1*}, A. ŁUKASZEK-SOLEK¹, T. ŚLEBODA¹, Ł. LISIECKI¹**EFFECT OF DEFORMATION OF Ti-3Al-8V-6Cr-4Zr-4Mo ALLOY UNDER VARYING THERMO-MECHANICAL CONDITIONS ON ITS MICROSTRUCTURE AND DEFORMATION BEHAVIOR**

This paper analyses the impact of thermomechanical processing history on the microstructure and thermomechanical behavior of Ti-3Al-8V-6Cr-4Zr-4Mo titanium alloy. The alloy was deformed in compression at various temperatures and strain rates, and the flow stress curves were elaborated basing on the testing data. The analysis of the material behavior at different temperature and strain rate ranges was performed taking into account various criteria of stability and instability of the material flow (Semiatiin-Lahoti criterion and Murty's criterion) under various thermomechanical conditions. It was shown, that the inhomogeneity of the alloy's microstructure in the initial state, mainly due to its crystallization conditions, is also a significant factor that affects the inhomogeneity of deformation. The study indicates that the analyzed alloy needs to undergo heat treatment to homogenize its structure before it can be subjected to processing. The processing maps developed using both the Semiatiin-Lahoti and Murty criteria were found to be effective in predicting flow instability and optimising hot forming parameters. The maps highlighted regions susceptible to adiabatic shear bands and strain localisation, while also identifying optimal conditions for dynamic recrystallisation and material softening. The results of this study may have direct applications in the design of thermomechanical processing of the studied titanium alloy under industrial conditions.

Keywords: Titanium alloy; thermo-mechanical processing; processing maps

Introduction

Titanium alloys represent a particularly significant subset of engineering materials. Distinguished from other materials by their remarkable properties, titanium alloys have found applications in a multitude of industries [1,2]. Titanium β alloys are frequently employed in the manufacture of aircraft landing gear, fuselages, wings and other load-bearing or loaded components [3]. Consequently, the alloy must possess excellent workability and microstructure. It is noteworthy that the Ti-3Al-8V-6Cr-4Zr-4Mo alloy exhibits high strength and relatively high ductility. Furthermore, it is distinguished by its higher corrosion resistance compared to other high-strength titanium alloys, and maintains its strength properties at temperatures up to 350°C. Furthermore, this β -Ti alloy displays a high susceptibility to forging above the β -transus temperature. Additionally, the Ti-3Al-8V-6Cr-4Mo-4Zr alloy's microstructure evolves significantly during aging treatments, influencing both its mechanical properties and its resistance to deformation, which is critical for optimizing its performance in high-demand applications [4].

An extremely important processing method for titanium alloys is thermomechanical processing (TMP) [5,6] during which phenomena such as dynamic recrystallisation (DRX) [7], dynamic globalisation [8], dynamic phase transition [9], texture evolution [10] or dynamic recovery (DRV) occur. They have a significant effect on the deformation behaviour of the material during hot processes. Furthermore, the mechanical properties of titanium alloys are quite sensitive to the evolution of the microstructure, which depends on the processing parameters, including strain temperature, strain rate and deformation. Therefore, in the pursuit of satisfactory microstructure and properties, the determination of reasonable hot processing parameters plays an essential role in the manufacturing process. Microstructures formed during thermomechanical machining are not easily altered by subsequent heat treatment due to the strong microstructural inheritance of Ti alloys [11]. Traditionally, many materials researchers have made efforts to optimise the processing parameters of alloys by conducting trial and error experiments and developing a theoretical model that has been helpful in understanding the mechanism of hot deformation [12-15].

¹ AGH UNIVERSITY OF KRAKOW, FACULTY OF METALS ENGINEERING AND INDUSTRIAL COMPUTER SCIENCE, AL. A. MICKIEWICZA 30, 30-059 KRAKOW, POLAND

* Corresponding author: stomasik@agh.edu.pl



Hot processing parameters cannot be easily controlled during hot deformation processes. Therefore, an important element in the design and control of the material's deformation behaviour is the use of processing maps [16].

A processing map is a representation of the material's response in terms of microstructural changes to imposed process parameters. Proposed by Prasad et al. [17,18], processing maps are constructed by superimposing the material flow instability map and the energy dispersion map, which are developed from the Dynamic Material Model (DMM).

Power dissipation efficiency (η) describes the constitutive response of a workpiece in terms of the different microstructural mechanisms operating at a given temperature and strain rate. The variation of η with temperature and strain rate provides a power dissipation map depicting the different domains that can be directly correlated with specific microstructural mechanisms. The η parameter is expressed by the following Eq. (1):

$$\eta = \frac{J}{J_{\max}} = 2 \left(1 - \frac{1}{\sigma \dot{\epsilon}_0} \int \sigma d\dot{\epsilon} \right) \quad (1)$$

Where J is dissipator co-content (component related to power dissipation through structural changes, e.g. dynamic recrystallization, dynamic recovery, grain growth), $J = J_{\max} = \frac{P}{2} = \frac{\sigma \dot{\epsilon}}{2}$ for the ideal linear dissipator ($m = 1$), σ is stress, and $\dot{\epsilon}$ is strain rate.

In order to identify areas of plastic flow instability in the development of the processing maps, it is necessary to consider the flow instability criterion [19]. Currently, the most commonly used instability criteria are those proposed by Prasad and Murty. In Prasad's instability criterion, the exponent of sensitivity to strain rate m , which is an important parameter defining the power split between heat generation and microstructure changes and is expressed by the Eq. (2):

$$m = \left(\frac{\partial \log \sigma}{\partial \log \dot{\epsilon}} \right)_{T, \epsilon} \quad (2)$$

Where T is temperature, ϵ is strain, and $\dot{\epsilon}$ is strain rate.

It is considered constant and independent of the strain rate. Murty, on the other hand, suggested that the parameter m cannot be considered as a constant value and therefore in his works [20-22] proposed a simpler and more stringent criterion for flow instability (ξ) than Prasad, which is expressed as follows:

$$\xi = \frac{2m}{\eta} - 1 \quad (3)$$

The variation of the ξ parameter with temperature and strain rate creates an instability map. Typical microstructural manifestations of flow instability are the formation of adiabatic shear bands, flow localisation, dynamic strain ageing, mechanical twinning and flow collapse or rotation.

Processing maps have been used to study the hot machinability and deformation mechanism of many other β -alloys, and it has been confirmed that DRV and DRX are the dominant deformation mechanisms in stable areas [23].

A phenomenological criterion was proposed by Semiatin and Lahoti for predicting flow localization phenomena [24,25]. Flow localization may occur during hot deformation in the absence of frictional and chilling effects, resulting from flow softening. In axisymmetric deformation states (such as upsetting), flow localization manifests as localized bulges on the workpiece. The phenomenon of flow softening, also known as negative work hardening, can be attributed to several factors, including structural instabilities such as adiabatic heating, the development of a softer texture during deformation, grain coarsening, and spheroidization. The appearance of flow localisation is typically characterised by curved or wavy macroscopic bands oriented at approximately 35-45° with respect to the principal stress axis. The flow localization parameter (α) is a function of material properties and can be expressed as:

$$\alpha = -\frac{\gamma}{m} \quad (4)$$

where: m – the strain rate sensitivity parameter, γ – the normalized flow softening rate expressed as:

$$\gamma = \frac{1}{\sigma} \frac{\partial \sigma}{\partial \epsilon} = \frac{\partial \ln \sigma}{\partial \epsilon} \quad (5)$$

This flow localization parameter can be utilized to estimate the tendency of a material to form pronounced or catastrophic strain concentrations. The Semiatin and Lahoti criterion is an empirical formula that shows good agreement with experimental results in titanium alloys. Flow localization will occur when the parameter α is greater than or equal to 5.

The instability parameter based upon the flow localization concepts could be expressed as:

$$\xi_1 = 1 - \frac{\alpha}{5} < 0 \quad (6)$$

The processing map is an effective tool for predicting flow instability, optimising process parameters, assessing the material's susceptibility to hot working and controlling microstructure evolution [26], therefore, the present study investigated the effect of thermomechanical processing history on microstructure changes in Ti-3Al-8V-6Cr-4Zr-4Mo titanium alloy. The alloy was deformed over a wide range of temperature and strain rates, and then process maps were constructed based on Murty's criterion. For characterizing material instability in thermomechanical deformation process in the case of titanium alloy, the analysis of the flow localization parameter α for a true strain in the range of 0.1-0.9 was also conducted. The maps of distribution of the parameter α , based upon the flow localisation concepts of Semiatin and Lahoti, were presented only for the cases in which $\alpha > 5$.

Experimental procedures

The chemical composition of the investigated alloy (wt.%) is shown in TABLE 1. Ti-3Al-8V-6Cr-4Mo-4Zr alloy, also known as Beta C or ASTM Grade 19, which is a high-temperature

Chemical composition of Ti-3Al-8V-6Cr-4Mo-4Zr alloy

Composition	C	V	Cr	Mo	Zr	Al	Fe	O	N	Y	Ti
Content, %	0.014	8.2	6.4	4.2	4.1	3.5	0.08	0.08	0.009	0.005	Bal.

alloy containing β -phase stabilising elements (V, Cr, Mo, Fe) [2], was investigated in the study.

Uniaxial compression tests were carried out using a Gleeble thermomechanical simulator to determine the influence of the hot processing parameters and the microstructural changes in the investigated Ti alloy being a result of hot processing. Axisymmetric specimens of 10 mm in diameter and 12 mm in height were cut out parallel to the axis of the rolled Ti alloy bar, which was the starting material. The specimens were then heated at the heating rate of 2.5°C/s for 10 s. Uniaxial compression tests were carried out over a wide temperature range of 800-1100°C at different strain rates in the range of 0.01-100 s⁻¹ up to true strain of 0.9.

A detailed examination and analysis of the microstructures was undertaken, with particular attention paid to the verification of the processing maps. The microstructure was analysed using a Leica DM4000M light microscope. The specimen's subsequent state, resulting from the deformation tests conducted under varying thermo-mechanical parameters, was then subjected to the analysis. The microstructures of tested samples were observed within the central area of the cross-sections of the specimens, in a plane aligned with the direction of compression.

Results

The investigated alloy at as-delivered condition was in a form of a rod of diameter of 100 mm (cast, rolled, solution treated and aged). The initial microstructure of the investigated material, as illustrated in Fig. 1, is characterised by the presence of a narrow, finely-crystallised zone of frozen crystals, and two distinct regions of dendrites and an interdendritic zones. The formation of the frozen crystal zone can be attributed to the rapid cooling and solution heat treatment and ageing resulted in the dispersion of α precipitates.

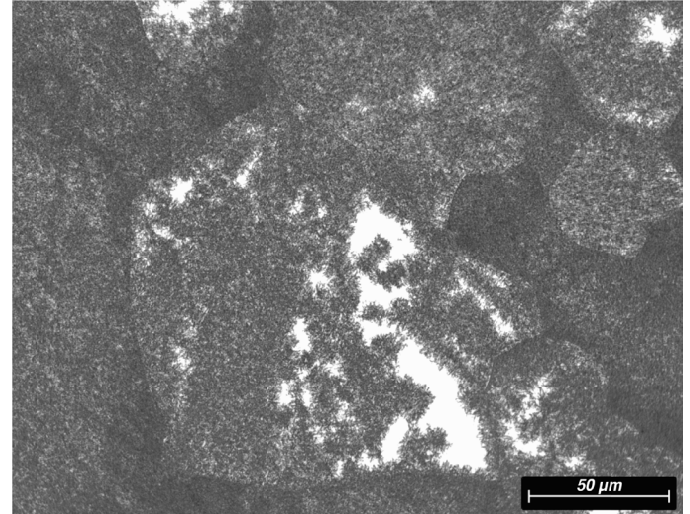


Fig. 1. Microstructure of Ti-3Al-8V-6Cr-4Mo-4Zr alloy in delivery condition

TABLE 2 illustrates the stress values for strain rates between 0.01 and 100 s⁻¹ within the specified temperature range of 800 to 1100°C.

As can be seen in TABLE 1, a decrease in stress is observed when the strain temperature increases and the strain rate decreases. The initial increase in stress in all tasted temperatures is due to strain hardening, while the subsequent decrease is due to material softening. This suggests an increase in dislocation density during the initial phase of deformation [27].

It should be noted that the reduction in the level of stress during the material flow may be attributed to mechanisms such as dynamic recrystallisation (DRX), dynamic recovery (DRV), and superplasticity [28]. However, it may also be linked to unstable material flow.

TABLE 2

Stress values for strain range of 0.1-0.9, strain rates of 0.01 s⁻¹ and 100 s⁻¹ and temperatures in the range of 800-1100°C

ϵ	0.1	0.2	0.3	0.4	0.5	0.6	0.7	0.8	0.9
T (°C)	$\dot{\epsilon} = 0.01 \text{ s}^{-1}$								
800	141.9	141.2	137.3	134.5	130.8	127.8	119.8	113.8	111.7
900	74.1	72.1	70.5	68.3	67.0	64.8	62.6	62.6	63.7
950	54.6	51.6	51.0	51.5	54.0	53.9	53.8	55.1	58.2
1000	41.4	39.0	38.1	38.3	37.3	37.4	38.4	40.9	43.4
1100	29.1	28.7	27.5	26.9	25.3	26.9	26.9	26.7	26.8
T (°C)	$\dot{\epsilon} = 100 \text{ s}^{-1}$								
800	567.5	588.3	601.8	607.2	603.3	589.3	555.5	507.7	460.4
900	436.1	429.4	428.0	428.0	425.5	422.5	410.8	386.3	366.9
950	365.6	359.2	357.3	356.7	354.8	350.2	341.1	323.8	298.5
1000	327.7	322.9	317.6	319.1	317.1	312.1	302.8	289.1	266.6
1100	267.1	259.5	256.3	254.8	253.2	250.2	244.0	232.4	220.7

Processing maps in accordance with Semiatiin-Lahoti criterion

The characterisation of material instability in the thermomechanical deformation of Grade 19 titanium alloy was achieved through the analysis of the flow localisation parameter α for true strains ranging from 0.1 to 0.9. The Fig. 2 presents the α distribution maps, based on the flow localisation concepts of Semiatiin and Lahoti, for cases where $\alpha > 5$. The isocline distribution of parameter α indicates that the material deforms non-uniformly across the entire cross-section.

The map of the flow localisation parameter α for the true strain of 0.9 shown one irregular area of instability. Area is situated within the following contour of the parameters: $T=800-1075^\circ\text{C}$, $\dot{\epsilon}=0.6-100\text{ s}^{-1}$, and it includes parameter $\alpha > 5$. The configuration and disposition of the isoclines of parameter α may indicate a deficiency in technological plasticity, accom-

panied by a high degree of deformation and a growing level of strain rate within the specified temperature range. The character of the instability can be analysed to identify that no softening of the metal occurs. However, the only phenomenon that does occur is that of strain, and the results of dynamic recrystallisation can also be observed. The observations of microstructures demonstrate the complete development of dynamic recrystallisation throughout the entire volume of the sample, as well as the reconstruction of the internal crystal structure.

The observations presented allow us to conclude that the formation of adiabatic shear bands is not a defect of flow instability in the entire range of process temperatures ($800-1100^\circ\text{C}$) and strain rates ($0.01-100\text{ s}^{-1}$). In order to fully comprehend the occurrence of adiabatic shear bands and the subsequent formation of cracks, it is essential to consider the underlying mechanisms and conditions that differentiate them from those observed in the context of dynamic recrystallization and dynamic recovery. The

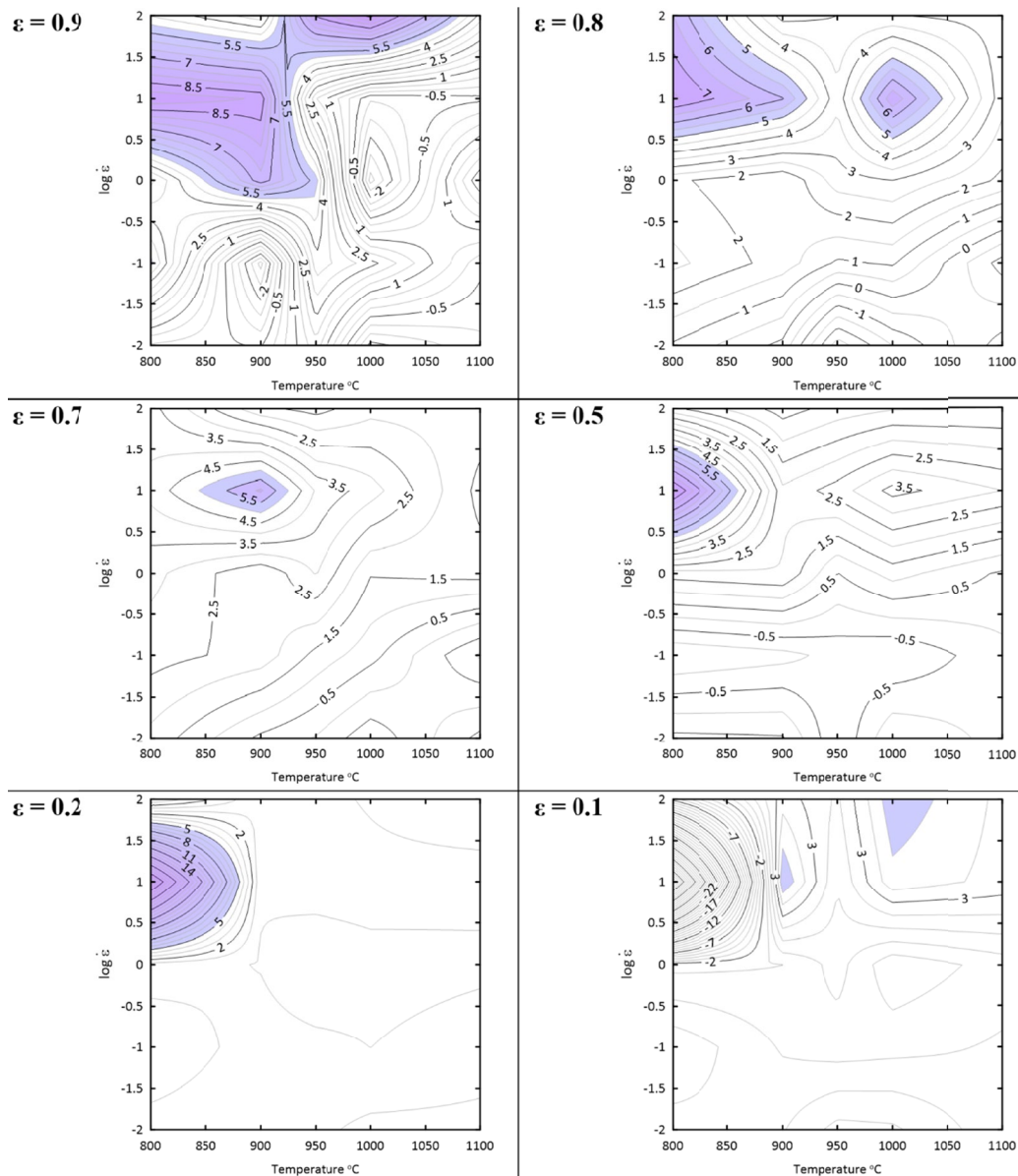


Fig. 2. Maps based upon flow localisation criterion (parameter α) for the Ti-3Al-8V-6Cr-4Mo-4Zr alloy at the true strain of: 0.9, 0.8, 0.7, 0.5, 0.2, 0.1; purple colour – instability area

deformation process may be applicable to conventional conditions, where the regions of intensive deformation (for example, a high strain rate and the gradient of temperature) and the produced adiabatic deformation heat will include the boundaries of phases between the adjacent areas of discontinuous deformation. This may result in the formation of a two-phase structure of alloys.

The map of the flow localization parameter α for $\varepsilon = 0.8$ shows the two most likely areas of instability. *Area I* is situated within the following contour of the parameters: $T = 800\text{-}925^\circ\text{C}$, $\dot{\varepsilon} = 3.2\text{-}100\text{ s}^{-1}$. The analysis of the character of that instability does not demonstrate the effect of flow softening of metal in the case of an excessively low process temperature. It may, however, indicate the non-uniform material flow resistance in different directions, together with an increase in strain rate. *Area II* includes process parameters: $T = 975\text{-}1050^\circ\text{C}$, $\dot{\varepsilon} = 3.2\text{-}31.6\text{ s}^{-1}$ and includes parameter $\alpha > 5$. Simultaneously with a decrease in strain, no areas of process instability occur only for the true strains of 0.6, 0.4, 0.3 ($\alpha < 5$). In the case of the true strain of 0.7, 0.5 and 0.2 on the flow localization map in one area situated in the case of the following parameters: the temperature range is $850\text{-}925^\circ\text{C}$, with a strain rate of $5.6\text{-}17.8\text{ s}^{-1}$ ($\varepsilon = 0.7$) and for $\varepsilon = 0.5$ – the temperature range is $800\text{-}875^\circ\text{C}$, $\dot{\varepsilon} = 3.2\text{-}31.6\text{ s}^{-1}$, and for the true strain 0.2 – the with a strain rate of $1.86\text{-}56.2\text{ s}^{-1}$. The parameter α is greater than 5. This area is composed of arranged isoclines, which have the shape of an arc in the direction of increasing temperature and decreasing strain rate. The presented observations provide confirmation that the maximum material flow softening occurs in the case of very slow deformation and the longtime of material exposure at a high temperature. The flow localization map at $\varepsilon = 0.1$ illustrates the stability area, which is characterized by a highly dense arrangement of isoclines. These isoclines exhibit the shape of an arc. Additionally, the map depicts the two small areas of instability, which is described by the parameters $T = 890\text{-}910^\circ\text{C}$ and $\dot{\varepsilon} = 6.3\text{-}25\text{ s}^{-1}$ and $T = 990\text{-}1040^\circ\text{C}$ and $\dot{\varepsilon} = 17.8\text{-}100\text{ s}^{-1}$, for $\alpha > 5$.

Moreover, the locations of strains can be correlated with both high strain rates and low thermal conductivity of titanium alloys. Metal forming at high strain rates results in low heat dissipation due to the deformation of the alloy, which has a low thermal conductivity, and the short process time. Consequently, the deformation process carried out under such conditions leads to a reduction in local flow stresses and may result in the occurrence of strain localisation bands (adiabatic shear bands). Conversely, high strain rates result in the accumulation of energy due to the lack of time for dissipation or the continuous generation of dislocations.

Processing maps in accordance with Murty's criterion

The determination of the parameters associated with metal forming requires a high level of precision, as these exert a profound influence on the mechanical properties and microstructure of the resulting products. During hot metal forming, alterations in the material's microstructure have a significant impact on the

quality of the finished product. The control of the microstructure and the prediction of the material's behaviour with respect to temperature, strain rate and true strain value during hot forming are of the utmost importance when designing the optimal conditions to implement metal forming processes. The distribution of power dissipation efficiency (η) is represented as a map, which is dependent on the change in strain rate, temperature and strain. Such a map illustrates the changes in energy dissipation resulting from the evolution of the microstructure. Higher values of η correspond to favourable parameters of hot deformation, as they reflect the large amount of energy dissipated due to the evolution of the microstructure. The variation of the instability parameter with temperature and strain rate led to the creation of an instability map, which can be superimposed on the power dissipation map to obtain a processing map. A negative value of this parameter may be indicative of the potential for flow instabilities to occur during deformation. These instabilities may be associated with the formation of strain-localised zones, adiabatic shear bands, cracking, or Lüders bands.

The processing maps were constructed in accordance with Murty's criterion. The isolines illustrate the distribution of the power dissipation efficiency parameter, η , while the shaded areas of instability are associated with a negative value of the parameter, ζ . The true strain values were 0.1, 0.2, 0.5, 0.7, 0.8 and 0.9 (Fig. 3). Maps generated by Semiatin's criterion, which exhibited areas of instability, were constructed for identical true strain values. The distribution of isolines suggests that a reduction in strain rate correlates with an increase in the efficiency of energy dissipation. It can be observed that the maximum values of power dissipation efficiency (η) are concentrated in the areas with the lowest strain rates analysed. Areas with high values for the power dissipation efficiency parameter (also referred to as the η parameter) are often considered to describe favourable metal forming parameters of a material, as they are characterised by the occurrence of dynamic recrystallisation, dynamic recovery, and superplasticity. Dynamic recrystallisation, which is a mechanism that increases the plastic formability of a material, can be referred to as the phenomenon whereby the material exhibits the ability to recrystallize under dynamic conditions. The values of power dissipation efficiency that are necessary for the occurrence of dynamic recrystallisation are considered to be in the range of 30-50%, while values above 60% can be related to superplasticity. The values of η (20-30%) are often associated with dynamic recovery. The maximum values of the energy dissipation efficiency ($\eta = 52\text{-}64\%$) are concentrated in the areas with the lowest strain rate (0.01 s^{-1}), which corresponds to a significant portion of the energy dissipated due to microstructural changes. The figure for true strain of 0.9 indicates that for the lowest strain rate of 0.01 s^{-1} and for the entire range of temperatures analysed, two regions with high energy dissipation efficiency values can be distinguished. In one of the ranges under investigation, a peak in the maximum value of the energy dissipation efficiency parameter is observed. The area with the maximum energy dissipation efficiency, equal to 64%, is observed at 900°C and a strain rate of 0.01 s^{-1} . This may suggest

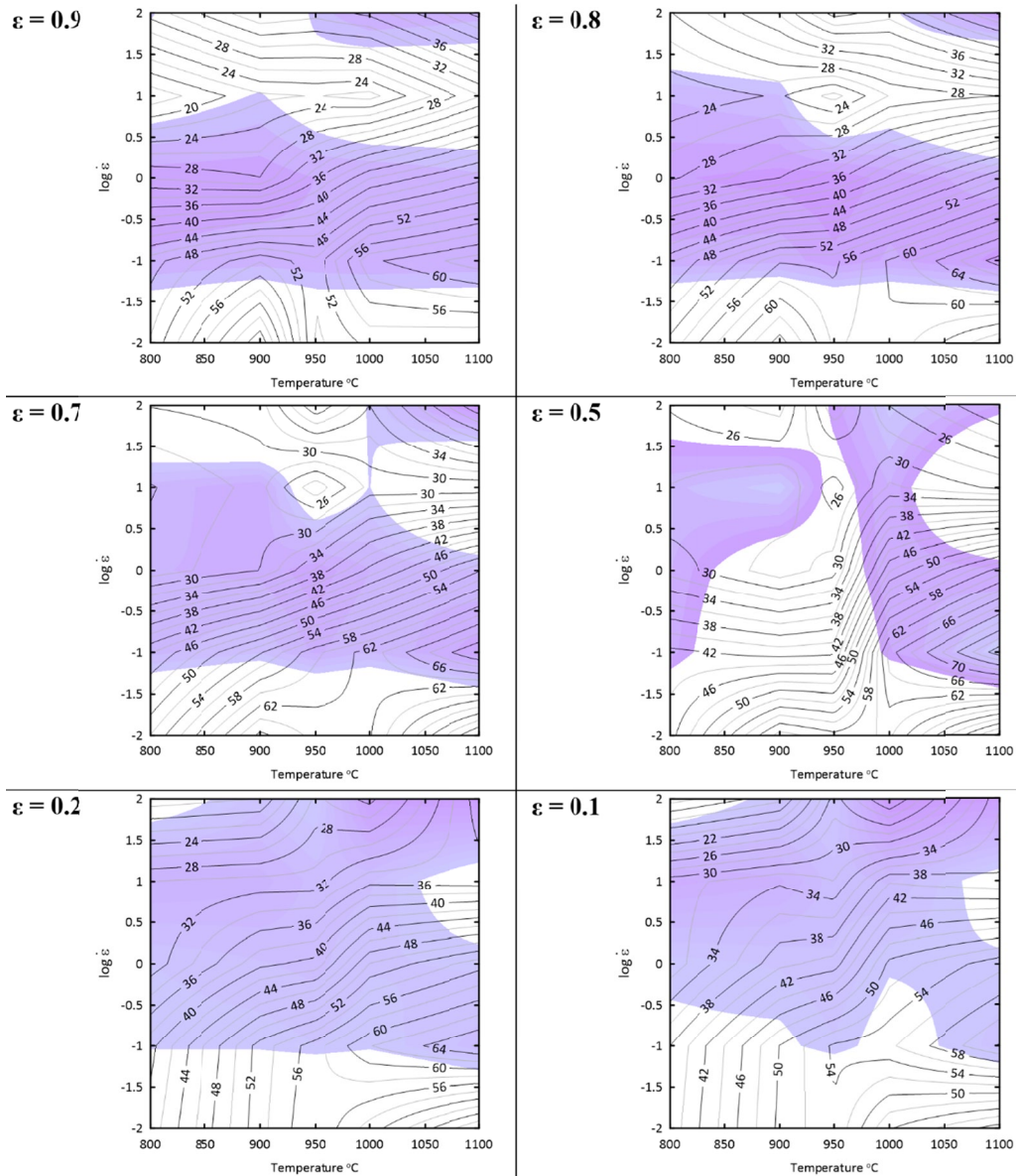


Fig. 3. The processing map of the Ti-3Al-8V-6Cr-4Mo-4Zr alloy at true strain of 0.1, 0.2, 0.5, 0.7, 0.8 and 0.9 as a function of temperature and strain rate, with shadowed unsafe domain

that this alloy can be shaped under superplastic conditions. The second area can be distinguished for temperatures in the range 950 to 1100°C, where the energy dissipation efficiency parameter takes values equal to or greater than 52%. These regions can be interpreted as representing dynamic recrystallization of the β -phase. The energy dissipation efficiency values are typically observed to range between 18 and 34% in the areas corresponding to the lowest temperatures analysed (800°C and 900°C) and the highest strain rates of 10 and 100 s^{-1} . This type of deformation behaviour can be associated with dynamic recovery.

A processing map for a true strain of 0.9 was created, with the differentiation of four processing windows. The processing windows that were identified as the most optimal were those that displayed significant parameters of the process and that included design recommendations for thermomechanical forging processes. The process window I occurs within the range of strain rates 18-100 s^{-1} and temperatures 800-925°C. In this area,

the energy dispersion parameter assumes values within the range 24-34%. This area can be associated with dynamic recovery. This is the most optimal area for hot deformation during hammer forging. In the context of the second process window, strain rates are observed to be relatively low, with values ranging from 0.01 to 0.03 s^{-1} . Furthermore, the plastic forming temperatures were found to be within the range of 800 to 950°C. It is noteworthy that the energy dissipation efficiency (η) exhibits values within the range of 50 to 64%. This observation can be interpreted as reflecting the highest susceptibility of the material to plastic deformation. It can thus be concluded with a high degree of probability that material deformation within the aforementioned range is likely to result in the occurrence of dynamic recrystallization or superplasticity. The third processing window may be identified within a temperature range of 950-1100°C and a strain rate of 0.01-0.03 s^{-1} . It is important to note that the efficiency of this process is approximately 58%. This phenomenon can be

attributed to the considerable dissipated energy involved in the evolution of the microstructure. The fourth process window for a true strain of 0.9 is distinguished by relatively low energy dissipation efficiency (η) values, with a range of 22-36%. The processing window can be identified at temperatures ranging from 950 to 1100°C and strain rates of 5.6 to 32 s⁻¹. In order to assess a material's hot formability based on processing maps, it is necessary to consider its hot deformation characteristics across a broad spectrum of applied strain values. This is particularly relevant in the context of the complex geometry of shaped parts, which gives rise to significant variations in the deformation values observed. Furthermore, it is important to note that as the strain values decrease, the positions and sizes of the processing windows also change. With regard to process windows I and IV, it should be noted that these disappear for strain values below 0.5. The results may be verified by analysing the microstructure of the materials deformed in accordance with the corresponding process maps.

Additionally, the two areas of instability (purple colour) for a true strain of 0.9 were identified. The extent of deformation is contingent upon the magnitude of the strain. Consequently, the

areas of flow instability exhibit a change in size and position as the strain changes. This phenomenon may be indicative of the material undergoing unstable deformation. For the smallest strain values, extensive areas of flow instability are observed, where $\zeta \leq 0$. It is advisable to avoid deformation parameters corresponding to areas of plastic flow instability.

Based on the processing maps of the investigated titanium alloy, it can be observed that the degree of deformation has a significant influence on the identification of the processing windows and the area of instability. This may be due to the continuous development of a microstructure during thermomechanical processing. For the true strains analysed, the processing maps constructed according to Murty's criterion clearly show increasingly larger areas of instability.

Analysis of microstructures

An examination of the microstructure of the investigated alloy after hot compression tests (Fig. 4) revealed that recryst-

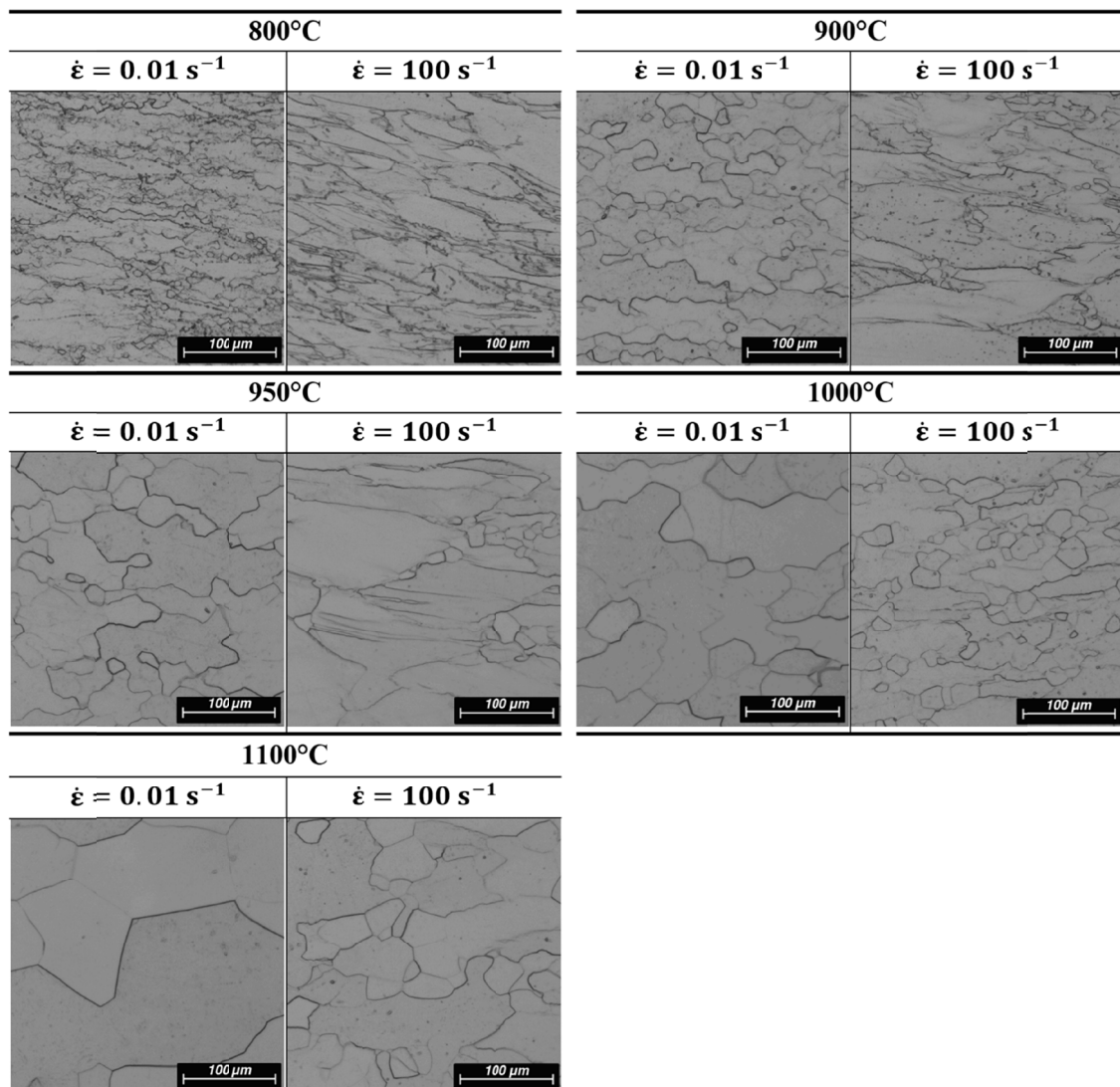


Fig. 4. The microstructure of the Ti-3Al-8V-6Cr-4Zr-4Mo alloy after plastic deformation at strain rate 0.01 s⁻¹ and 100 s⁻¹ and for temperatures of 800, 900, 950, 1000 and 1100°C

tallisation occurred during deformation for the majority of the parameters employed (at deformation temperatures exceeding 800°C). The formation of new equiaxial grains at the boundaries of the existing grains is evident. Furthermore, it can be observed that at both investigated strain rates at 800°C and 900°C, the grains display elongation in the direction transverse to the applied compressive force. In materials deformed at higher temperatures, the orientation of the grains is leveled as a result of the microstructural remodelling processes that occur (dynamic recrystallisation).

Conclusions

This study provides a comprehensive analysis of the impact of strain history and deformation conditions on the microstructure and deformation behaviour of the titanium alloy Ti-3Al-8V-6Cr-4Zr-4Mo. The findings offer valuable insights for optimising its processing. The research yielded the following conclusions:

- The study demonstrated that deformation at varying temperatures and strain amplitudes exerts a pronounced influence on the microstructure. In particular, dynamic recrystallisation (DRX) and dynamic recovery (DRV) mechanisms were observed to be significant during high-temperature deformation, exerting a considerable influence on the material's behaviour.
- The investigation corroborated the hypothesis that elevated deformation temperatures (exceeding 800°C) facilitate recrystallisation, thereby promoting the formation of new equiaxed grains. Lower strain rates and higher temperatures have been found to enhance microstructural uniformity, while higher strain rates have been observed to increase the probability of microstructural instability.
- The initial microstructural inhomogeneity of the alloy, largely attributable to the crystallisation conditions, was identified as a pivotal factor influencing the non-uniformity of deformation. The aforementioned inhomogeneity thus requires heat treatment prior to plastic processing, with the objective of achieving structural homogenisation and enhanced deformation consistency.
- The processing maps developed using both the Semiatin-Lahoti and Murty criteria were found to be effective in predicting flow instability and optimising hot forming parameters. The maps highlighted regions susceptible to adiabatic shear bands and strain localisation, while also identifying optimal conditions for dynamic recrystallisation and material softening.

Acknowledgements

The research was funded by the Ministry of Education and Science through the AGH research subvention under contract number 16.16.110.663 (task 3 and 13).

REFERENCES

- [1] Q. Zhao et al., High-strength titanium alloys for aerospace engineering applications: A review on melting-forging process. *Materials Science and Engineering: A* **845**, 143260, Jun. (2022). DOI: <https://doi.org/10.1016/j.msea.2022.143260>
- [2] F.N. Ahmad, H. Zuhailawati, A Brief Review on the Properties of Titanium as a Metallic Biomaterials. *IJEM* **8**, 63-67, Sep. (2020).
- [3] S.K. Kar, A. Ghosh, N. Fulzele, A. Bhattacharjee, Quantitative microstructural characterization of a near beta Ti alloy, Ti-5553 under different processing conditions. *Materials Characterization* **81**, 37-48, Jul. (2013). DOI: <https://doi.org/10.1016/j.matchar.2013.03.016>
- [4] S.-W. Lee, H.-M. Kim, Y.-J. Lee, J.-G. Lee, D.-G. Lee, Effect of Aging Treatment on the Microstructure and Mechanical Properties of Ti-3Al-8V-6Cr-4Mo-4Zr Alloy. *Appl. Sci.* **14**, 14, 6192, Jul. (2024). DOI: <https://doi.org/10.3390/app14146192>
- [5] C. Wu, L. Huang, C.M. Li, Experimental investigation on dynamic phase transformation and texture evolution of Ti55531 high strength titanium alloy during hot compression in the $\alpha+\beta$ region. *Materials Science and Engineering: A* **773**, 138851, Jan. (2020). DOI: <https://doi.org/10.1016/j.msea.2019.138851>
- [6] H. Yang et al., Some advances in plastic forming technologies of titanium alloys. *Procedia Engineering* **81**, 44-53 (2014). DOI: <https://doi.org/10.1016/j.proeng.2014.09.127>
- [7] X. Chen et al., Dynamic recrystallization and hot processing map of Ti-48Al-2Cr-2Nb alloy during the hot deformation. *Materials Characterization* **179**, 111332, Sep. (2021). DOI: <https://doi.org/10.1016/j.matchar.2021.111332>
- [8] S. Long et al., Constitutive modelling, dynamic globularization behavior and processing map for Ti-6Cr-5Mo-5V-4Al alloy during hot deformation. *J. Alloys Compd.* **796**, 65-76, Aug. (2019). DOI: <https://doi.org/10.1016/j.jallcom.2019.05.031>
- [9] Y. Li, S. Ni, Y. Liu, M. Song, Phase transition induced high strength and large ductility of a hot rolled near β Ti-5Al-5Mo-5V-1Cr-1Fe alloy. *Scr. Mater.* **170**, 34-37, Sep. (2019). DOI: <https://doi.org/10.1016/j.scriptamat.2019.05.031>
- [10] J. Krawczyk, Ł. Frocisz, M. Goły, S. Tomasiak, T. Śleboda, The Analysis of Changes in the Crystal Structure of Near-Beta Titanium Alloy in the Solution-Treated and Aged Conditions after Static Tensile Testing. *Crystals* **13**, 8, 1223, Aug. (2023). DOI: <https://doi.org/10.3390/cryst13081223>
- [11] G. Lütjering, J.C. Williams, *Titanium*. Berlin, Heidelberg: Springer Berlin Heidelberg (2003).
- [12] X. Bao, W. Chen, J. Zhang, Y. Yue, J. Sun, Achieving high strength-ductility synergy in a hierarchical structured metastable β -titanium alloy using through-transus forging. *Journal of Materials Research and Technology* **11**, 1622-1636, Mar. (2021). DOI: <https://doi.org/10.1016/j.jmrt.2021.02.012>
- [13] S. Shi, J. Ge, Y.C. Lin, X. Zhang, K. Zhou, High-temperature deformation behavior and recrystallization mechanism of a near beta titanium alloy Ti-55511 in β phase region. *Materials Science and Engineering A* **847**, 143335, Jul. (2022). DOI: <https://doi.org/10.1016/j.msea.2022.143335>

- [14] C. Li, L. Huang, M. Zhao, S. Guo, Y. Su, J. Li, Systematic analysis of the softening mechanism and texture evolution of Ti–6Cr–5Mo–5V–4Al alloy during hot compression in $\alpha+\beta$ phase region. *Materials Science and Engineering A* **850**, 143571, Aug. (2022). DOI: <https://doi.org/10.1016/j.msea.2022.143571>
- [15] T. Lu et al., Flow softening and microstructural evolution of near β titanium alloy Ti-35421 during hot compression deformation in the $\alpha+\beta$ region. *Journal of Materials Research and Technology* **19**, 2274, Jul. (2022). DOI: <https://doi.org/10.1016/j.jmrt.2022.05.144>
- [16] R.J. Immanuel, S.K. Panigrahi, J.C. Malas, Materials development for sustainable manufacturing. in *Sustainable Manufacturing Processes*, Elsevier, 2023, p. 155-194.
- [17] Y.V.R.K. Prasad, Processing maps: A status report. *J. Mater. Eng. Perform.* **12**, 6, 638-645, Dec. (2003). DOI: <https://doi.org/10.1361/105994903322692420>
- [18] Y.V.R.K. Prasad, T. Seshacharyulu, Processing maps for hot working of titanium alloys. *Materials Science and Engineering: A* **243**, 1-2, 82-88, Mar. (1998). DOI: [https://doi.org/10.1016/S0921-5093\(97\)00782-X](https://doi.org/10.1016/S0921-5093(97)00782-X)
- [19] M. Xiong, Z. Weidong, S. Yu, Z. Yongqing, W. Shaoli, Z. Yigang, A comparative study of various flow instability criteria in processing map. *Rare Metal Materials and Engineering* **39**, 5, 756-761, May (2010). DOI: [https://doi.org/10.1016/S1875-5372\(10\)60096-3](https://doi.org/10.1016/S1875-5372(10)60096-3)
- [20] S.V.S.N. Murty, B.N. Rao, On the development of instability criteria during hotworking with reference to IN 718. *Materials Science and Engineering A* **254**, 1-2, 76-82, Oct. (1998). DOI: [https://doi.org/10.1016/S0921-5093\(98\)00764-3](https://doi.org/10.1016/S0921-5093(98)00764-3)
- [21] S.V.S. Narayana Murty, M.S. Sarma, B.N. Rao, On the evaluation of efficiency parameters in processing maps. *Metall. and Mat. Trans. A* **28**, 7, 1581-1582, Jul. (1997). DOI: <https://doi.org/10.1007/s11661-997-0219-y>
- [22] S.V.S.N. Murty, B.N. Rao, Instability map for hot working of 6061 Al-10 vol% metal matrix composite. *J. Phys. D Appl. Phys.* **31**, 22, 3306-3311, Nov. (1998). DOI: <https://doi.org/10.1088/0022-3727/31/22/020>
- [23] Z. Hu, X. Zhou, H. Liu, D. Yi, The formation of microtextured region during thermo-mechanical processing in a near- β titanium alloy Ti-5Al-5Mo-5V-1Cr-1Fe. *J. Alloys Compd.* **853**, 156964, Feb. (2021). DOI: <https://doi.org/10.1016/j.jallcom.2020.156964>
- [24] Y.H. Mozumder, K.A. Babu, S. Mandal, Compressive Flow Behaviour and Deformation Instabilities of Fe-Mn-Al-Ni-C Lightweight Duplex Steel. *Trans. Indian Natl. Acad. Eng.* **5**, 3, 465-474, Sep. (2020). DOI: <https://doi.org/10.1007/s41403-020-00105-x>
- [25] M. Wan, F. Li, K. Yao, G. Song, X. Fan, Theory, method and practice of metal deformation instability: A review. *Materials (Basel)* **16**, 7, Mar. (2023). DOI: <https://doi.org/10.3390/ma16072667>
- [26] S. Liu, Q. Hu, F. Zhao, X. Chu, Utilization of steel slag, iron tailings and fly ash as aggregates to prepare a polymer-modified waterproof mortar with a core-shell styrene-acrylic copolymer as the modifier. *Constr. Build. Mater.* **72**, 15-22, Dec. (2014). DOI: <https://doi.org/10.1016/j.conbuildmat.2014.09.016>
- [27] E. Ghasemi, A. Zarei-Hanzaki, E. Farabi, K. Tesař, A. Jäger, M. Rezaee, Flow softening and dynamic recrystallization behavior of BT9 titanium alloy: A study using process map development. *J. Alloys Compd.* **695**, 1706-1718, Feb. (2017). DOI: <https://doi.org/10.1016/j.jallcom.2016.10.322>
- [28] J. Sieniawski, M. Motyka, Superplasticity in titanium alloys. *Journal of Achievements in Materials and Manufacturing Engineering* **24**, 1, 123-130 (2007).